DOI: 10.26599/FSHW.2026.9250991

Contents lists available at SciOpen

Food Science and Human Wellness

journal homepage: https://www.sciopen.com/journal/2097-0765

China Food Publishing Co.

Protective effect of polysaccharide from *Sargassum fusiforme* against UVB-induced skin barrier damage in HaCaT cells and BALB/c hairless mice

Jiachen Liang[#], Lijuan Deng[#], Yifan Chen, Huamai Qiu, Abdul Mueed, Lijun You*

School of Food Science and Engineering, South China University of Technology, Guangzhou, Guangdong, 510640, People's Republic of China

Research Institute for Food Nutrition and Human Health (111 Center), Guangzhou, Guangdong, 510640, People's Republic of China

ABSTRACT: Excessive ultraviolet B (UVB) exposure disrupt the skin barrier, provoking inflammation. This study investigated the protective effects of a degraded *Sargassum fusiforme* polysaccharide (DSFP-45) against UVB-induced barrier dysfunction in HaCaT keratinocytes and BALB/c nude mice. DSFP-45 significantly improved cell viability, reduced reactive oxygen species, and restored barrier-protiens (filaggrin, loricrin, and aquaporin 3) in UVB-irradiated HaCaT cells. It suppressed pro-inflammatory cytokines (TNF-α, IL-1β, and IL-6) by inhibiting the PI3K/Akt/NF-κB pathway. *In vivo*, oral and topical DSFP-45 alleviated erythema, reduced transepidermal water loss, preserved collagen and elastic fibers, normalized ceramide levels, and suppressed pro-inflammatory cytokines (TNF-α, IL-1β, and IL-6). The 16s rRNA sequencing showed that DSFP-45 increased beneficial skin microbiota (*Staphylococcus* and *Lactobacillus*), and reduced harmful taxa (*Corynebacterium*, *Streptococcus*, and *Stenotrophomonas*). Kyoto Encyclopedia of Genes and Genomes (KEGG) metabolic pathway analysis showed that the skin microbiota under DSFP-45 treatment influence biosynthesis of amino acids and biosynthesis of secondary metabolites. These findings demonstrate that DSFP-45 protected against UVB-induced skin barrier damage by enhancing barrier protein expression, dampening inflammation, and possibly by modulating skin microbiota, supporting its potential as a natural anti-photodamage agent.

Keywords: *Sargassum fusiforme* polysaccharide; UVB-induced photodamage; Skin inflammation relief; Skin barrier repair function; Skin microbiota modification; PI3K/Akt/NF-κB pathway.

1. Introduction

The skin is the body largest organ and serves as the primary barrier against environmental stressors, including ultraviolet (UV) radiation. Among UV wavelength, UVB (280-315) penetrates the epidermis and induces significant biomolecular damage, such as protein denaturation, lipid oxidation, and DNA lesions. These effects lead to excessive production of reactive oxygen species (ROS), triggering inflammation, collagen degradation, and disruption of barrier integrity[1], which clinically manifests as erythema, dryness, wrinkle formation and accelerated photoaging. Prolonged or repeated UVB exposure also contributes to the development of skin cancers[2, 3].

# These two authors contributed equally to this manuscript.
Corresponding author
Prof. Lijun You, E-mail: feyoulijun@scut.edu.cn

Received 18 September 2025
Received in revised from 3 October 2025
Accepted 27 October 2025

An intact skin barrier relies on structural proteins such as filaggrin, involucrin, loricrin, tohether with natural moisturing factors and intercellular lipids. A critical feature of UVB-induced vicious cycle of inflammation and skin barrier impairment. Initially, UVB exposure leads to barrier disruption and inflammatory responses. Under the thermal stress of UVB irradiation, the intercellular junctions of the stratum corneum may be compromised due to dehydration. UVB-induced ROS generation further damages proteins closely associated with skin barrier function[4], characterized by reduced level of structural proteins such as filaggrin, involucrin, loricrin, along with increased transepidermal water loss (TEWL). Meanwhile, ROS production triggers oxidative stress, while DNA damage activates NOD-like receptor (NLRP) inflammasomes, leading to inflammation, characterized by increased secretion of pro-inflammatory cytokines, including interleukin (IL)-1β, IL-6, and Tumor Necrosis Factor (TNF)-α[1]. Subsequently, barrier impairment exacerbates inflammatory responses, while inflammation hinders barrier recovery. A disrupted barrier facilitates the penetration of immunogenic substances, thereby aggravating inflammation[5]. Moreover, opportunistic pathogens can further amplify cutaneous inflammation under barrier-compromised conditions, and in severe cases, even cause bacterial infections[6, 7]. Inflammatory cytokines suppress the synthesis of barrier-associated proteins[8]. Thus, perpetuating a self-reinforcing cycle of inflammation and barrier dysfunction. Modulating the phosphoinositide 3-kinase/protein kinase B/nuclear factor kappa B (PI3K/Akt/NF-κB) signaling pathway, a key regulator of inflammatory cytikines including TNF-α, IL-1β, and IL-6[7], repairing skin barrier, and restoring skin flora is therefore a promising strategy to attenuate UVB-mediated skin injury.

Seaweed-derived polysaccharides have attracted increasing attention as natural bioactive agents because of their antioxidant, anti-inflammatory and immunomodulatory activities[9]. In particular, polysaccharides extracted form *Sargassum fusiforme* exhibit various biological activities, including antioxidant[10], enhancing immunity[11], anti-tumor[12], anti-photoaging[13], hypoglycemic[14]. The backbone of *Sargassum fusiforme* polysaccharides was →4)-β-ManA-(1→4)-α-GulA-(1→4)-β-ManA-(1→4)-β-ManA-(1→4)-α-GulA-(1→4)-β-ManA-(1→3,4)-β-ManA-(1→, and the terminal group α-Fucp-(1→ was linked to the main chain via O-3 position of →3,4)-β-ManA-(1→[15]. *Sargassum fusiforme* polysaccharides exhibits structural similarities to alginic acid with a long main chain and few branches. Our previous work demonstrated that a degraded *Sargassum fusiforme* polysaccharide prepared by UV/H_2O_2 treatment for 45 minutes (DSFP-45), whose structure was elaborated in our previous study, possesses enhanced solubility and antiphotoaging activity[16]. However, its protective effects against UVB-induced skin barrier dysfunction and the underlying mechanism remain unclear. Notably, DSFP-45 was shown to alleviate chronic photoaging by modulating the transforming growth factor-β/Smad (TGF-β/Smad) signaling pathway and suppressing matrix metalloproteinases (MMPs)[17]. Therefore, we hypothesized that DSFP-45 protects against UVB-induced skin barrier damage by enhancing barrier-related protein expression, reducing inflammatory cytokine secretion, and modulating the skin microbiota. Also this study aimed to investiagate the ability of DSFP-45 to protect against UVB-induced skin

barrier damage in HaCaT keratinocytes and BALB/c nude mice. we focused on barrier-related protein expression, inflammatory cytokines regulation through the PI3/Akt/NF-kB signaling pathway, and alteration in skin microbiota, to provide mechanistic insight into the anti-photodamage potential of DSFP-45.

2. Materials and methods

2.1 Materials

Sargassum fusiform was collected from Dongtou District, Wenzhou, Zhejiang, China. *Sargassum fusiform* superfine powder was obtained after the sample was washed, dried, sheared and followed by superfine comminution using XDW-6BI grinder (Jinan Tatsu Micro Machinery Co. Ltd., Jinan, Shandong, China) and passed through a 40 mesh sieve (particle size ≤ 0.4 mm).

DMEM, penicillin-streptomycin, FBS, phosphate-buffered saline (PBS) and other reagents for cell culture were purchased from Gibco Biotechnology Co., Ltd. (Grand Island, NY, USA). Hyaluronic acid(HA) (97%, 200-400 kDa) was obtained from Shanghai Macklin Biochemical Co., Ltd. (Shanghai, China). TRIzol reagent was purchased from Vazyme Biotech Co., Ltd. (Nanjing, Jiangsu, China). The cDNA Synthesis was purchased from Tsingke Biotechnology Co., Ltd. (Beijing, China). Primers of genes were obtained from Sangon Biotech Co., Ltd. (Shanghai, China). All other reagents and chemicals used were of analytical grade. filaggrin (FLG), aquaporin-3 (AQP3), loricrin (LOR) and Ceramide ELISA kit were acquired from Wuhan Fine Biotech Co., Ltd. (Wuhan, China). SDS-PAGE was purchased from Wuhan Affinity Biosciences Co. Ltd （Wuhan, Hubei, China). PVDF was purchased from Thermo Fisher Scientific Co. Ltd (Waltham, Massachusetts, USA). GAPDH and IL-1β primary antibodies and secondary antibodies was purchased from Wuhan Servicebio Technology Co., Ltd. (Wuhan, Hubei, China). BCA Protein Assay Kit was purchased from Shanghai Biyuntian Biological Co., Ltd (Shanghai, China).

2.2 Extraction and degradation of polysaccharides from Sargassum fusiforme

Polysaccharides from *Sargassum fusiforme* was extracted by the reported method in our previous study. Specifically, the *Sargassum fusiforme* powder was decolorized three times with 95% ethanol (1:4, w/v) for 4 h each, followed by hot water extraction at 100 °C for 4 h (1:50, w/v). After filtration and centrifugation at 8000 r/min for 15 min, the supernatant was concentrated to one-tenth of its original volume. Crude polysaccharide was subsequently precipitated with 80% ethanol overnight and lyophilized. A 2% *Sargassum fusiforme* polysaccharide solution prepared from the powder was then subjected to UV irradiation (HOPE-MED 8140, Tianjin Hepu Industry & Trade Co. Ltd., Tianjin, China) at 950 μW/cm^2 for 45min. After degradation, manganese dioxide (MnO_2) was added immediately and magnetically stirred for 12 h. The solution was concentrated to 1/5 of its initial volume at 60 °C using a reduced rotary evaporator (Hei-VAP Value Digital, Heidoph, Nuremberg, Germany). For MnO_2, the supernatant was removed by centrifugation (12000 × g, 5 min), followed by purification via dialysis (3 kDa molecular weight cut-off) for 48 h. Finally, the retentate was collected, concentrated by evaporation, and vacuum freeze-dried (Alpha 1–2 LD Plus, Martin Christ

Gefriertrocknungsanlagen GmbH, Osterode am Harz, Germany) to obtain the degradation product, named as DSFP-45[17].

2.3 Skin Barrier Repair Activity of DSFP-45 in vitro

2.3.1 Cell culture and viability assay

Human immortalized epidermal cells (HaCaT), purchased from the Chinese Academy of Medical Sciences, were seeded in DMEM complete medium (containing 10% FBS, 1% penicillin and streptomycin) and cultured in a constant temperature incubator containing 5% CO_2 at 37℃. MTT assay was used to detect cell viability.

2.3.3 Cell Pretreatment and Determination of FLG, AQP3, LOR, TNF-α and IL-6 level

The cells were cultured in DMEM complete medium in six well plates for 12h, and then cultured in serum-free medium for 12h (5×10^5 cells/well). Next, the cells were treated with serum-free medium co

ntaining different concentrations of polysaccharides (62.5, 125, and 250 μg/mL) for 6 h, followed by irradiation (2 mJ/cm², 24 h).

Cells were lysed in 300 μL of lysis buffer on ice for 40 min, followed by centrifugation (12000 × g, 4°C, 15 min). The resulting supernatant was collected. The BCA protein kit wasused to determine the protein content. According to the kit's in-structions, the supernatants were then used to measure contents of FLG, LOR, AQP3, TNF-αand IL-6.

2.3.4 Determination of ROS level

The cell modeling method was performed as 2.2.3. After modeling, the PBS was discarded, and 100 μL of DCFH-DA probe diluted in DMEM basal medium (at a ratio of 1:250) was added to each well. Following a 30-minute incubation in a cell culture incubator, excess probe that had not entered the cells was washed away. Then, 100 μL of PBS was added to each well, and the fluorescence intensity was measured. The ratio of the absorbance value of each well to that of the control well was calculated to evaluate the effect of DSFP-45 on intracellular ROS levels in HaCaT cells after UVB irradiation.

2.3.5 Determination of IL-1β level

HaCaT cells were seeded into 60 mm culture dishes at a density of 1.5×10^6 cells per well. The cell modeling procedure was performed as previously described. After washing each well twice with 1 mL of PBS, 400 μL of lysis buffer was added, and the cells were lysed on ice for 20 min. Subsequently, cells were scraped using a cell scraper, transferred into centrifuge tubes, and further lysed on ice for an additional 20 min. The lysates were then centrifuged at 12,000 × g for 20 min at 4°C, and the supernatant was collected into fresh centrifuge tubes. Protein samples were separated by SDS-PAGE and transferred onto PVDF. GAPDH and IL-1β antibodies (rabbit, 1:1000) were used as primary antibodies, followed by incubation with HRP-conjugated secondary antibody (goat anti-rabbit IgG, 1:2000). Protein bands were visualized, and densitometric analysis was performed using ImageJ software.

2.3.6 Quantitative Reverse Transcription–Polymerase Chain Reaction (qRT-PCR) Analysis

The cell supernatant was aspirated, and each well was washed twice with 1 mL PBS. The plates were then stored at −80°C for subsequent extraction of total cellular RNA. Total cell RNA was extracted with Trizol solution, reverse transcribed according to the instructions of Evo m-mlv reverse transcription kit and then analyzed by real-time fluorescent quantitative PCR. The expression level of the target gene was calculated by the relative quantitative $2^{-\Delta\Delta CT}$ method. The primer sequences of the main target genes were shown in Supplementary Material Table 1.

2.4 Skin Barrier Repair Activity of DSFP-45 in nude mice

2.4.1 Experimental grouping

Female BALB/c nude mice weighing 20 ± 2 g were purchased from Zhuhai Bestone Biotechnology Co., Ltd. (animal license No.: scxk- (Guangdong) 2020-0051). The animal experiment was carried out in the standardized SPF animal room of the experimental animal center of South China Agricultural University (the unit use license number is syxk (Guangdong) 2024-0136). After one week of adaptive feeding, 70 BALB/c nude mice were randomly divided into seven groups, with 10 mice in each group, including Control group, Model group, Positive control group, DSFP-45-L group, DSFP-45-M group, DSFP-45-H group and DSFP-45-smoothed group.

The experimental period lasted seven weeks. During the experiment, the solution was prepared at the ratio of 0.1 mL/10 g body weight every day. From week 1 to 7, the Control and Model groups were given distilled water by gavage, while the positive control group received hyaluronic acid (150 mg/kg/day). The DSFP-45 treatment groups included low- (75 mg/kg/day), medium- (150 mg/kg/day), and high-dose (300 mg/kg/day) oral administrations, along with a topical application group (300 mg/kg/day). During weeks 2–7, all groups except the Control underwent dorsal irradiation four times weekly (Monday, Wednesday, Friday, Sunday) 1 h post-treatment; the weekly dose was increased stepwise (200, 300, 400, 400, 500, 600 mJ/cm^2), reaching a cumulative total of 9.6 J/cm^2.

2.4.2 Measurement of skin TWEL of nude mice

Before the mice were dissected, the TWEL of nude mice skin were evaluated by measuring the TWEL of nude mice skin with a transdermal water shunt loss meter. The probe of the instrument was contacted with the skin surface of mice, and each mouse was measured three times to take the average value.

2.4.3 Elastica van Gieson (EVG) staining of nude mouse skin

The skin tissue was fixed in 4% paraformaldehyde, dehydrate using graded ethanol and soaked in wax, embedded, trimmed, sectioned, dried and stored at room temperature. The paraffin sections were dewaxed to water, stained, dehydrated rapidly with absolute ethanol after washing, xylene was transparent and neutral gum was wet sealed. The sections were placed under the microscope for microscopic examination (200 X).

2.4.4 Determination of pro-inflammatory cytokines, ceramide and barrier function protein content

A total of 100 mg of intestinal tissue was homogenized in 1 mL of PBS, with each sample prepared in triplicate. The homogenates were centrifuged(12000 × g, 4°C, 20 min), and the resulting supernatants were

collected and stored at −80°C. The protein concentration in the supernatants was determined using a BCA protein assay kit. Subsequently, the FLG, AQP3, LOR, IVL, ceramide, TNF-α, IL-1β, and IL-6 in the supernatants were measured according to the manufacturer's instructions of the respective assay kits. The results were normalized to the total protein content.

2.4.5 Quantitative Reverse Transcription–Polymerase Chain Reaction (qRT-PCR) Analysis

20 mg skin tissue mixed with 1 mL PBS and three 3 mm grinding beads in a enzyme-free homogenization tube, and then it was placed in a high-speed low-temperature tissue grinder for homogenization. The homogenization frequency is 60 Hz, the temperature is -10℃, pause for 30 s every 60 s and homogenize 10 times. The skin tissue RNA was extracted according to the kit instructions, and the purity and concentration of RNA were determined using a micro nucleic acid and protein analyzer. Reverse transcription was performed according to the instructions of Evo m-mlv reverse transcription kit, followed by real-time fluorescence quantitative analysis. The expression level of the target gene was calculated by the relative quantitative $2^{-\Delta\Delta CT}$ method. The primer sequences of the main target genes were shown in Supplementary Material Table 2.

2.4.6 Skin flora analysis

Mouse skin flora was collected before the end of the experiment. The sterile absorbent cotton was swabbed in sterile normal saline, and the it was wiped on the back of the mouse to collect the skin flora. The cotton swab head was cut off and putted into a sterilized cryopreservation tube, snap freezze with liquid nitrogen. Mouse skin flora was sent to Shanghai Meiji Biomedical Technology Co., Ltd. for determination. The sequencing results of skin flora were analyzed on the meggitt biocloud platform.

2.5 Statistical analysis

The data results were expressed in the form of " mean ± standard " deviation, and graphpad prism 9 software was used for mapping and analysis. One-way ANOVA was employed for statistical analysis, followed by Duncan's multiple comparison test for post hoc analysis. Statistical significance was defined as an adjusted *p*-value below 0.05. The sequencing results of skin microbiota and KEGG were analyzed on the Meiji Bioinformatics Cloud Platform.

3. Results and Discussion

3.1 Effect of DSFP-45 on the viability and ROS contents of HaCaT cells

The safety and non-toxicity of the sample are prerequisites for the experiment. The safety concentration of DSFP-45 was evaluated by measuring the survival rate of HaCaT cells using the MTT method. As shown in Figure 1A, compared with Control group, the cell survival rate of the HA and DSFP-45 group at 62.5, 125, 250 μg/mL concentrations incubated for 6 h was greater than 80%, demonstrated that polysaccharide concentration up to 250 μg/mL didn't exhibit obvious cytotoxicity. Therefore, HA and DSFP-45 were deemed suitable for subsequent experiments. Next, cell viability and ROS levels of the cell treated with these compounds were evaluated. Figure 1B and C showed the impact of different concentrations of HA and

DSFP-45 on photodamaged HaCaT cells. Compared with the Control group, cells in the Model group exhibited a significant decrease in viability and a marked increase in ROS contents ($P < 0.01$). Notably, DSFP-45 treatment significantly improved cell viability and attenuated the intracellular ROS levels in UVB-exposed HaCaT cells ($P < 0.05$). ROS are generated by oxidative stress induced by UVB[18], and this process may leads to cell death. Polysaccharides, as antioxidants, reduce ROS levels[19] and thus decrease the number of cell deaths. The findings demonstrated a protective effect of DSFP-45 against UVB-induced photodamage, further supporting its potential as an anti-photodamage agent.

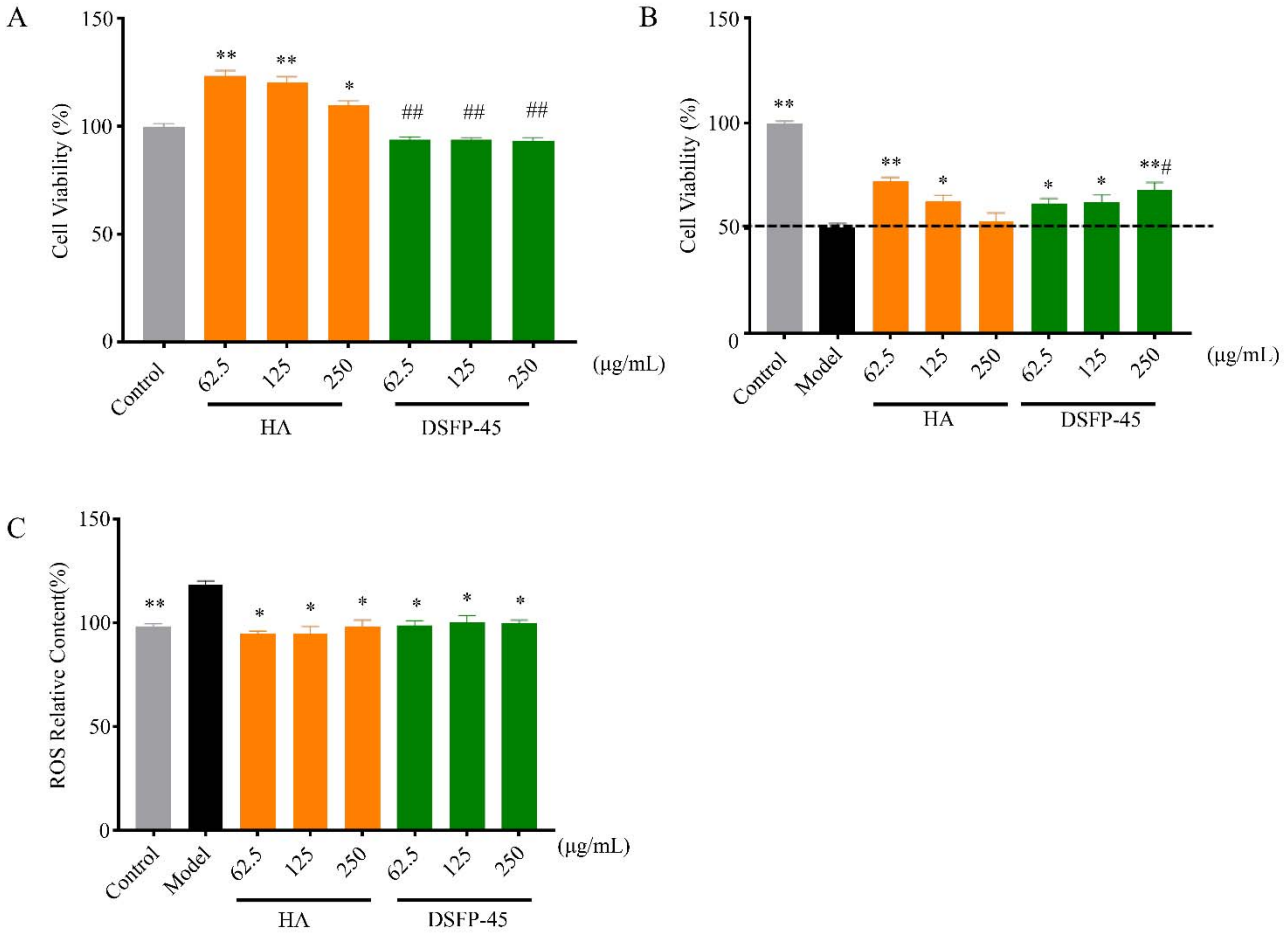

Figure 1. Effects of DSFP-45 treatment on the viabilities and ROS of HaCaT cells after UVB irradiation. (A) viabilities of non-irradiation; (B) viabilities of post-irradiation; (C) ROS contents.
Note: *, and ** indicate that other groups in the index have significant differences compared with the Model group.（$^{*}P < 0.05$, $^{**}P < 0.01$）. $^{\#}$, and $^{\#\#}$ indicate that other groups in the index have significant differences compared with group in same concentration.（$^{\#}P < 0.05$, $^{\#\#}P < 0.01$.

3.2 Effect of DSFP-45 on the contents and expression of barrier function proteins in HaCaT cells

The keratinized mantle is primarily composed of IVL, LOR and FLG, and its formation is regulated by transglutaminase 1. FLG is cleaved by calpain-1 and caspase-14 into filaggrin fragments, which are further degraded by bleomycin hydrolase, aminopeptidase and carboxypeptidase into natural moisturizing factors (NMF), such as trans-uric acid and 2-pyrrolidone carboxylic acid. NMF play critical roles in maintaining stratum corneum hydration, regulating skin pH and skin elasticity[20, 21]. Therefore, we analyzed the effect of DSFP-45 on skin barrier function using HaCaT cells.

The effects of DSFP-45 on FLG, LOR and AQP3 in UVB-induced damaged HaCaT cells are shown in Figure 2. Compared with the Control group, the Model group exhibited a significant decrease in both the contents and gene expression of FLG ($P < 0.05$), in the contents of LOR ($P < 0.05$), and in gene expression of IVL ($P < 0.05$), indicating that UVB irradiation impairs the skin barrier by reducing these key proteins. The relative expression level of the IVL gene was significantly increased compared with Control group ($P < 0.01$).Treatment with HA and DSFP-45 significantly restored FLG contents ($P < 0.05$) and expression ($P < 0.01$), LOR contents ($P < 0.05$) suggesting that DSFP-45 could promote the synthesis of barrier-related proteins and contributes to skin barrier repair.

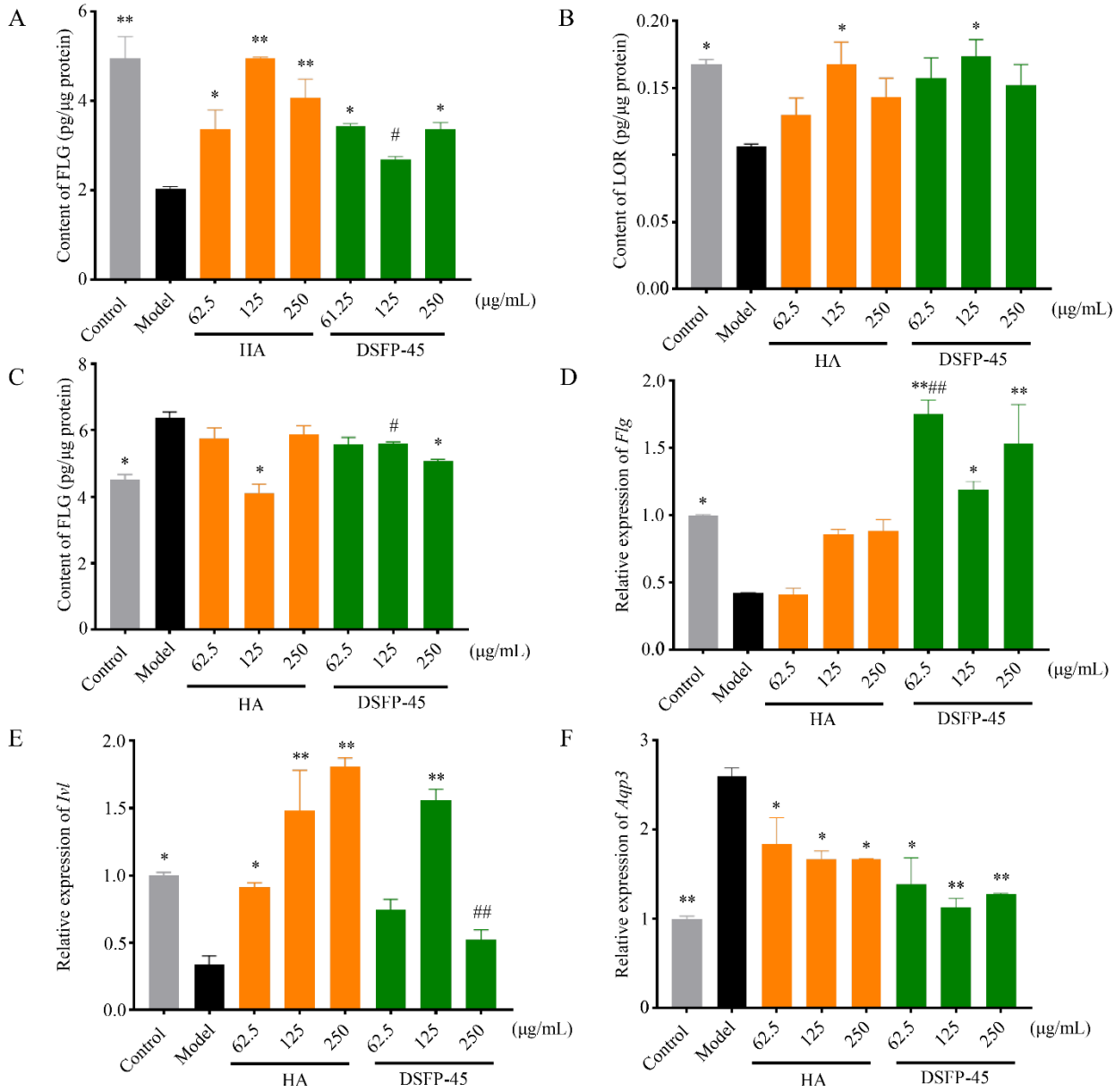

Figure 2. Effect of DSFP-45 on barrier function proteins of UVB-damaged HaCaT cells. (A) FLG contents; (B) LOR contents; (C) AQP3 contents; (D) *Flg* expression; (E) *Ivl* expression; (F) *Aqp3* expression.
Note: *, and ** indicate that other groups in the index have significant differences compared with the Model group.（$^{*}P < 0.05$, $^{**}P < 0.01$）. $^{\#}$, and $^{\#\#}$ indicate that other groups in the index have significant differences compared with group in same concentration.（$^{\#}P < 0.05$, $^{\#\#}P < 0.01$.

AQP3, a transmembrane water channel protein predominantly expressed in the skin, facilitating water transport and maintains epidermal hydration and homeostasis[22]. UVB-irradiation significantly increased

AQP3 content and gene expression in HaCaT cells ($P < 0.01$), likely as a compensatory response to barrier disruption and reduced water retention. After treatment with HA and DSFP-45 reversed this effect, lowering AQP3 levels. Similar results were reported by Kang et al, who observed that UVB exposure increased AQP3 but decreased the HA receptor CD44 in HaCaT cells, after treatment with catfish skin collagen hydrolysate reduced AQP3 and enhanced CD44 expression, alleviating UVB-induced barrier damage in hairless mice[23]. In summary, DSFP-45 significantly alleviated UVB-induced damage to barrier-related proteins. As noted earlier, barrier damage permits exogenous substance or bacterial invasion, and thereby exacerbates inflammatory responses. Thus, its barrier repair effect inhibits barrier-deficiency-associated skin inflammation.

3.3 Effect of DSFP-45 on pro-inflammatory cytokines in HaCaT cells

Excessive UV radiation induces the accumulation of ROS in the skin, thereby promoting the secretion of pro-inflammatory cytokines such as TNF-α, IL-1β, and IL-6. These cytokines impair the skin barrier through multiple mechanisms. For instance, TNF-α downregulates FLG and LOR in calcium-differentiated keratinocytes via activation of the c-Jun N-terminal kinase pathway[8]. Eri Sawada et al.[24] reported that IL-6 markedly reduces ceramide levels in the stratum corneum, accompanied by downregulation of genes encoding serine palmitoyltransferase-2, acidic sphingomyelinase, and β-glucocerebrosidase. Similarly, IL-1β disrupts terminal keratinocytes differentiation, leading to reduced FLG and LOR expression, diminished NMF content, Further compromising the barrier by inducing oxidative stress and amplifying inflammatory responses. Notably, Immunosuppressive agents, such as azathioprine, can alleviate this damage by suppressing IL-1β expression.[25]. To evaluate the anti-inflammatory effects of DSFP-45 on UVB-induced skin damage, HaCaT cells were treated with DSFP-45 and HA following UVB irradiation. The secretion levels and gene expression of pro-inflammatory cytokines (TNF-α, IL-6, and IL-1β), in HaCaT cells were subsequently quantified. As shown in Figure 3A-D), UVB irradiation significantly increased TNF-α ($P < 0.01$), IL-6 ($P < 0.01$), and IL-1β ($P < 0.05$) levels in the model group compared with the control group, confirming successful induction of photodamage. Treatment with different concentrations of DSFP-45 and HA markedly reduced cytokines secretion. Specifically, TNF-α levels were significantly decreased by 125 μg/mL DSFP-45 and 62.5 μg/mL HA ($P < 0.05$). IL-6 levels were reduced by DSFP-45 at 62.5, 125, and 250 μg/mL ($P < 0.05$), and by HA at 62.5 and 125 μg/mL ($P < 0.05$). In addition, IL-1β levels were significantly decreased by all tested concentrations of DSFP-45 and by 250 μg/mL HA ($P < 0.05$).

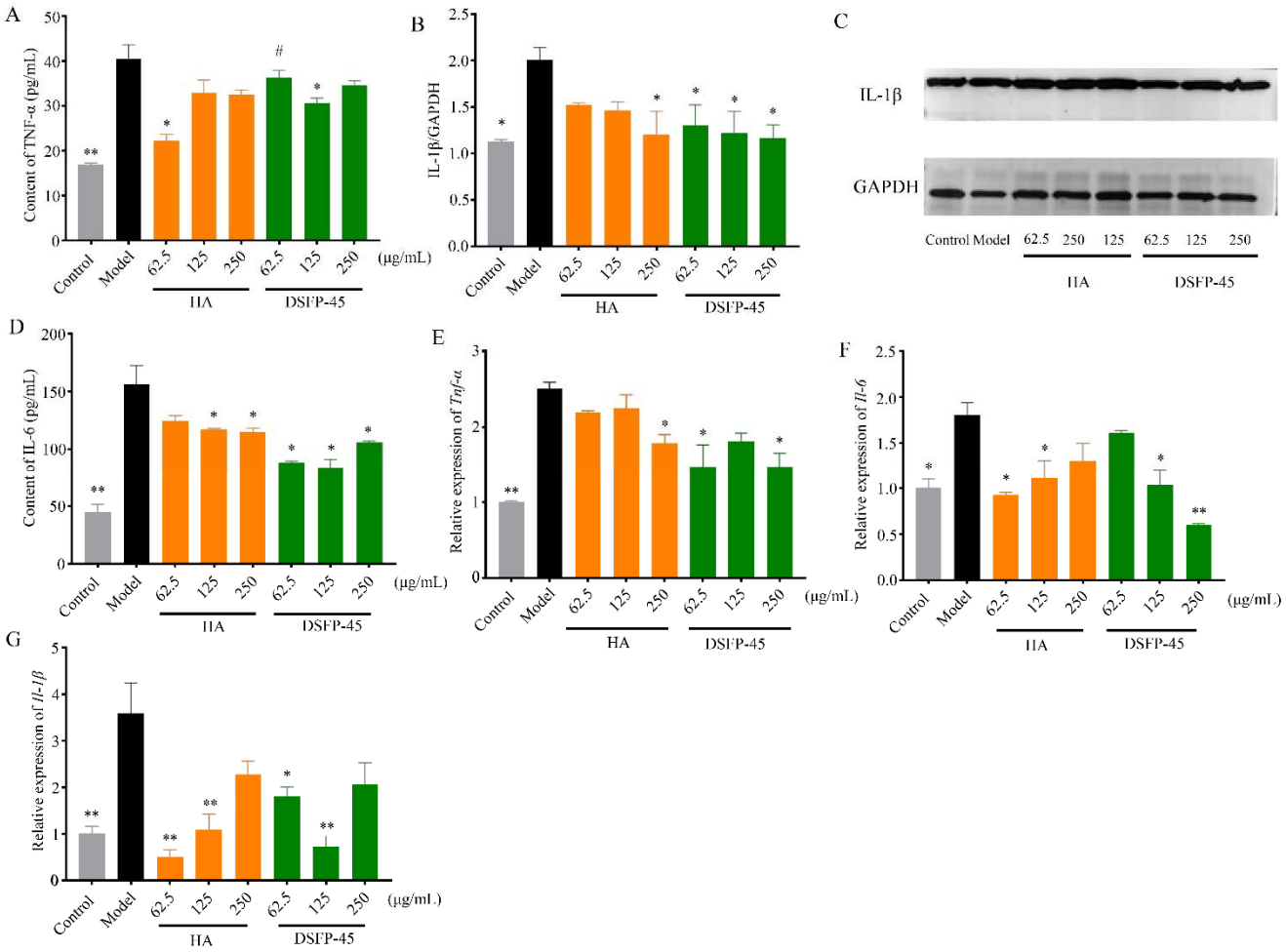

Figure 3. Effect of DSFP-45 on pro-inflammatory cytokines of UVB-damaged HaCaT cells. (A) TNF- α contents; (B) IL-6 contents; (C) IL-1β contents ; (D) Tnf- α expression; (G) Il-6 expression; (F) Il-1β expression.

Note: *, and ** indicate that other groups in the index have significant differences compared with the Model group.（$*P < 0.05$, $**P < 0.01$）. $^{\#}$, and $^{\#\#}$ indicate that other groups in the index have significant differences compared with group in same concentration.（$^{\#}P < 0.05$, $^{\#\#}P < 0.01$.

Gene expression analysis (Figure 3E-G), revealed that UVB irradiation significantly upregulated TNF-α, IL-1β, and IL-6 in the Model group compared to the Control group ($P < 0.05$), indicating that UVB exposure promotes the expression of pro-inflammatory cytokines. In contrast, treatment with HA and DSFP markedly suppressed the expression of these genes relative to the Model group. Specifically, following treatment with DSFP-45 at concentrations of 62.5, 125, and 250 μg/mL, the relative expression of TNF-α was reduced by 41.09%, 27.61%, and 41.24%, respectively; IL-1β by 49.70%, 79.95%, and 42.82%, respectively; IL-6 by 10.89%, 42.47%, and 66.57%, respectively. Collectively, these findings suggest that both DSFP-45 and HA effectively attenuate UVB-induced inflammation in HaCaT cells by downregulating the secretion and expression of key pro-inflammatory cytokines.

3.4 Effect of DSFP-45 on PI3K/AKT/NF-κB signaling pathway in HaCaT cells

Upon exposure to DNA-damaging environmental factors, such as UV radiation, or to aberrantly secreted cytokines from immune cells, the PI3K signaling is predominantly activated within the epidermis. Dysregulation of the cutaneous PI3K/AKT pathway is associated with pathological conditions characterized by uncontrolled keratinocyte proliferation[26]. Phosphorylation-induced Activation of AKT subsequently

triggers the NF-κB signaling cascade. This leads to dissociation of the inhibitor of IκB from NF-κB, facilitating NF-κB nuclear translocation and transcriptional activation of pro-inflammatory cytokines, thereby exacerbating cutaneous inflammation[27]. In the paper, HaCaT keratinocytes were pretreated with DSFP-45 or HA before UVB irradiation to evaluate the effects of DSFP-45 on PI3K/AKT/NF-κB signaling. As shown in Figure 4, UVB irradiation significantly evaluated the gene expression of Pi3k, Akt, and p65 in the model group compared with the Control group ($P < 0.05$), indicating that UVB irradiation promotes the expression of pro-inflammatory cytokines and induces skin inflammation. Treatment with HA and DSFP markedly downregulated the expression of these genes compared to the Model group. Specifically, DSFP-45 at 62.5, 125, and 250μg/mL reduced Pi3k expression by 37.04%, 73.76%, and 63.17%; Akt expression by 64.89%, 40.55%, and 27.93%, and p65 expression by 53.26%, 1.91%, and 32.42%, respectively. These results demonstrate that DSFP-45 exerts potent anti-inflammatory effects by suppressing activation of PI3K/AKT/NF-κB pathway, thereby attenuating UVB-induced cytokine expression. Collectively, these findings suggest that DSFP-45 can restore skin barrier function, inhibit inflammatory cytokine production, and disrupt the vicious cycle between skin barrier impairment and inflammation.

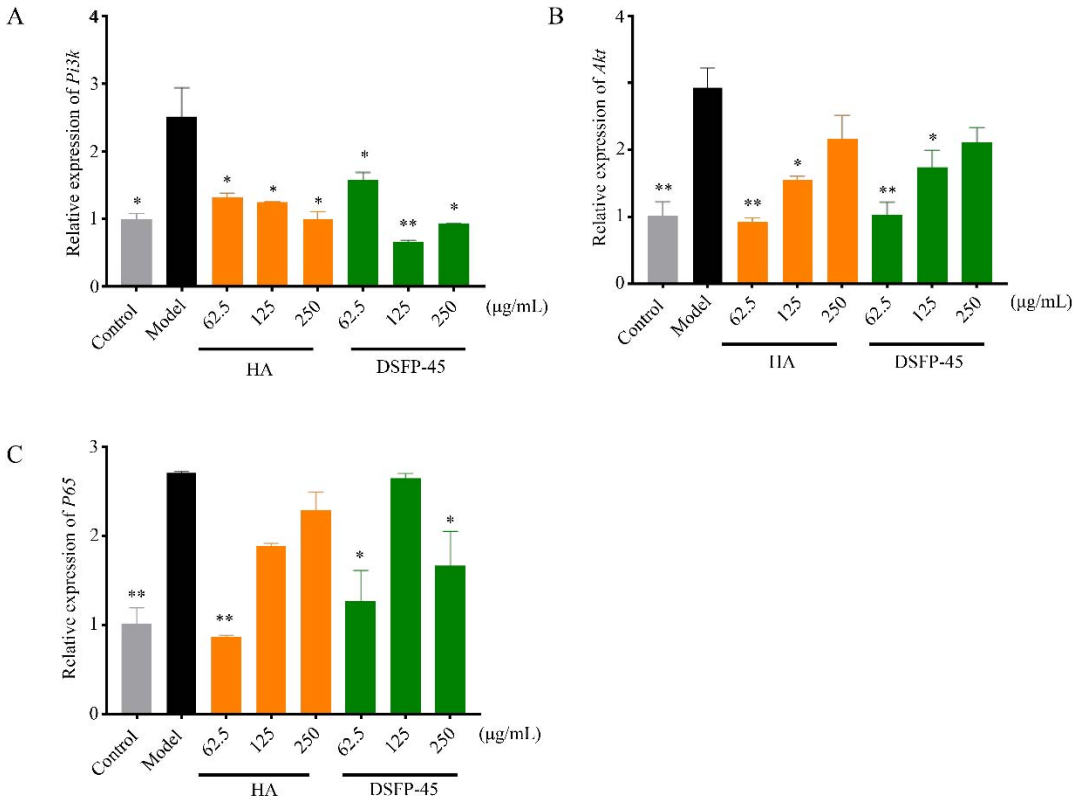

Figure 4. Effect of DSFP-45 on PI3K/AKT/NF-κB signaling pathway of UVB-damaged HaCaT cells. (A) Pi3k expression; (B) AKt expression; (C) P65 expression.
Note: *, and ** indicate that other groups in the index have significant differences compared with the Model group.（$*P < 0.05$, $**P < 0.01$）. $^{\#}$, and $^{\#\#}$ indicate that other groups in the index have significant differences compared with group in same concentration.（$^{\#}P < 0.05$, $^{\#\#}P < 0.01$.

3.5 Effect of DSFP-45 on skin and elastic fibers in photodamaged mice

As shown in Figure 5A, the skin of nude mice in the Control group appeared smooth, with fine texture and good elasticity. In contrast, the skin of mice in the Model group appeared rough and damaged, exhibiting

dryness, desquamation, erythema, and scabbing. These symptoms confirmed the successful establishment of the UVB-induced photodamage model, indicating significant disruption of the skin barrier and abnormal keratinization. Following oral administration and topical application of low and medium doses of DSFP-45, the scabbed areas were reduced and erythema and swelling were alleviated. Notably, treatment with HA and high-dose DSFP-45 almost completely restored the skin to a normal state, characterized by firmness, smoothness, and elasticity. These findings suggest that DSFP-45 and HA effectively protect the skin of nude mice by mitigating UVB-induced photodamage.

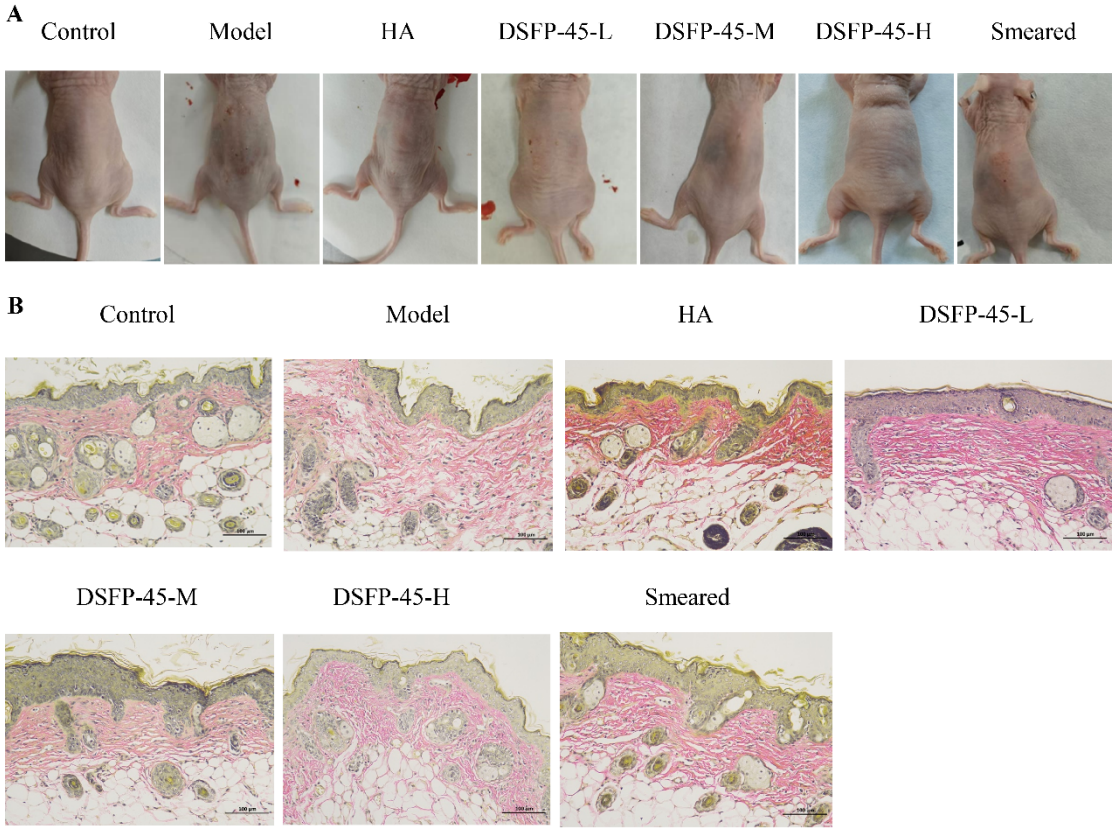

Figure 5. Effect of DSFP-45 on skin and elastic fibers in photodamaged mice. (A) skin; (B) elastic fibers.

Collagen fibers interweave with elastic fibers to form a mesh structure that supports and maintains skin. UVB irradiation caused epidermal thickening, fragmentation of dermal collagen fibers and deformation of elastic fibers in nude mice. The elevate the protective effect of DSFP-45, skin sections were subjected to EVG staining, in which elastic fibers appear purple-black and collagen fibers appear red. The results (Figure 5B) showed that the dorsal skin in the Control group mice contained evenly distributed elastic fibers with regular arrangement, while collagen fibers formed a well-organized mesh structure. In contrast, the Model group exhibited shrunken, rod-like elastic fibers that lost structural integrity and were disorganized, along with a reduced number of collagen fibers showing twisting and fragmentation. After treatment with HA and DSFP-45 restored elastic fibers morphology and significantly increased collagen fibers content increased with a more orderly arrangement. These results indicate that HA and DSFP-45 effectively inhibit UVB-induced elastic fibers deformation, promote collagen fibers synthesis and maintain the normal structure of the skin. Combined with the above data, the skin redness and loss of elastic fibers induced by UV irradiation indicated the successful establishment of the mice model. These phenomena are associated with the occurrence of

cellular inflammation[28]. Treatment with DSFP-45 can significantly improve skin conditions, demonstrating that DSFP-45 possesses potential anti-inflammatory activity.

3.6 Effect of DSFP-45 on skin barrier function in photodamaged mice

TEWL refers to the diffusion of water from the dermis through the epidermis and its evaporation from skin surface, Serving as a key indicator of stratum corneum barrier function[29]. Higher TEWL value indicate more water loss and impaired skin barrier integrity. In order to evaluate the skin barrier repair efficacy of DSFP-45 in photodamaged mice, the TEWL value of the dorsal skin of nude mice were measured using a VAPO SCAN probe. As shown in Figure 6A, TEWL values were significantly increased in the Model group following UVB irradiation compared with the control group ($P < 0.01$), confirming barrier disruption. After treatment with HA and DSFP-45 reduced TEWL, with significant improvements observed at medium and high doses, suggesting that DSFP-45 effectively repair the skin barrier and mitigates water loss. Similarly, Sim et al. reported that oral administration of rose petal extract decreased TEWL and inhibited collagen degradation, demonstrating pronounced anti-aging activity[30].

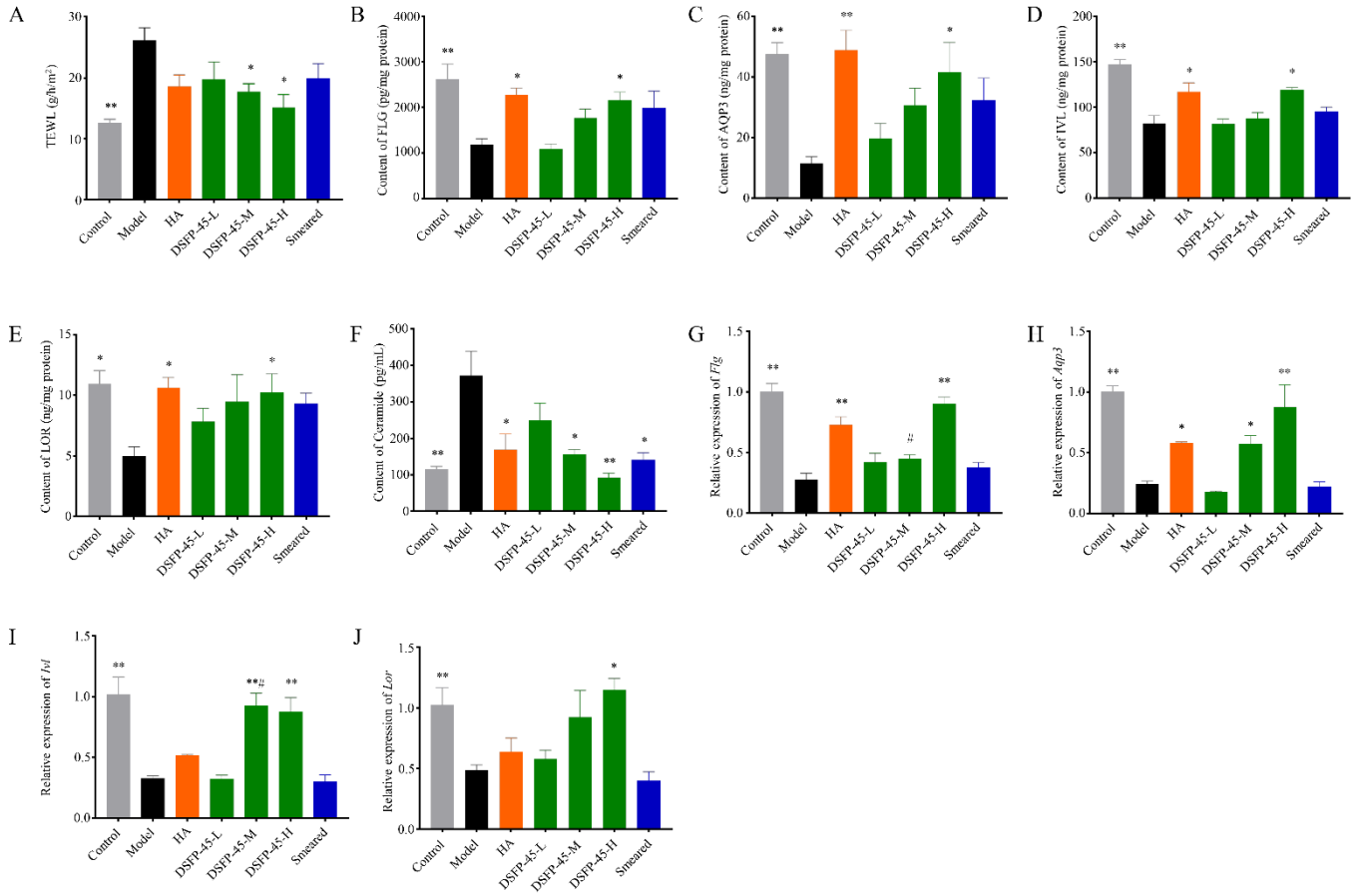

Figure 6. Effect of DSFP-45 on skin barrier function in photodamaged mice. (A)TEWL; (B) FLG contents; (C) AQP3 contents; (D) IVL contents; (E) LOR contents; (F) Cermide contents; (G) *Flg* expression; (H) *Aqp3* expression; (I) *Ivl* expression; (J) *Lor* expression.

Note: *, and ** indicate that other groups in the index have significant differences compared with the Model group. （$^{*}P < 0.05$, $^{**}P < 0.01$. $^{\#}$, and $^{\#\#}$ indicate that other groups in the index have significant differences compared with group in same concentration. （$^{\#}P < 0.05$, $^{\#\#}P < 0.01$.

The effect of DSFP-45 on skin barrier function proteins in photodamaged mice is shown in Figure 6B-J. Compared with the Control group, FLG, IVL, LOR and AQP3 levels were significantly decreased in the

Model group ($P < 0.05$), indicating that UVB irradiation downregulates barrier proteins, damage the skin barrier and aggravate photodamage. DSFP-45 treatment significantly restored the contents and gene expression of FLG, IVL, LOR and AQP3, thereby improved UVB-induced skin barrier dysfunction. Consistent findings were reported by Li et al, who found that ginsenoside treatment upregulated FLG, IVL and AQP3 expression in UVB irradiated mice skin, alleviated photoaging symptoms[31]. Notably, AQP3 shows an opposite trend in cells and animals. This phenomenon has been reported in numerous studies[32, 33], but its cause remains unclear. Studies indicate that UVB irradiation increases the proportion of mouse epidermal cells in the proliferative phase, with the peak appearing at 48h[34]. Meanwhile, repeated UVB exposure induces growth arrest in epithelial cells[35]. This suggests impaired proliferative repair capabilities as the irradiation dose increases. Specifically, low-dose UVB boosts the number of proliferative cells, while high-dose UVB reduces it. Additionally, epithelial cells in the proliferative phase have higher AQP3 levels than those in the terminal differentiation stage[36]. Combined with the AQP3 results from our cell and animal experiments, we infer that different UVB doses lead to changes in the number of proliferative cells, which in turn causes the opposite trends of AQP3.

In addition to NMF, intercellular lipids are critical for maintaining skin moisture. UVB irradiation has been shown to increase phosphatidylcholine and ceramide contents, while reducing sphingomyelin, driven by upregulated acidic sphingomyelinase activity, which accelerates phospholipid hydrolysis and ceramide formation, ultimately impairing barrier permeability and promoting intracellular water loss[37-39]. As shown in Figure 6F, compared with the Control group, ceramides content was significantly increased in the Model group ($P < 0.01$), which might provoke cell cycle arrest and apoptosis in cell types[38]. DSFP-45 treatment significantly reduced ceramide levels, indicating mitigation of UVB-induced cellular damage. Collectively, DSFP-45 exhibits strong anti-photodamage activity by restoring barrier functional proteins, normalizing AQP3 expression, and reducing ceramide accumulation, thereby improving overall skin barrier integrity.

3.7 Effect of DSFP-45 on pro-inflammatory cytokines in photodamaged mice

As shown in Figure 7A-C, the levels of pro-inflammatory cytokines (TNF-α, IL-1β, and IL-6) were significantly elevated in the skin of mice in the Model group compared with the Control group ($P < 0.05$), confirming that UVB irradiation promotes the production of pro-inflammatory cytokines and induces skin inflammation. Treatment with DSFP-45 or HA markedly reduced these cytokines levels ($P < 0.05$), indicating notable anti-inflammatory effects.

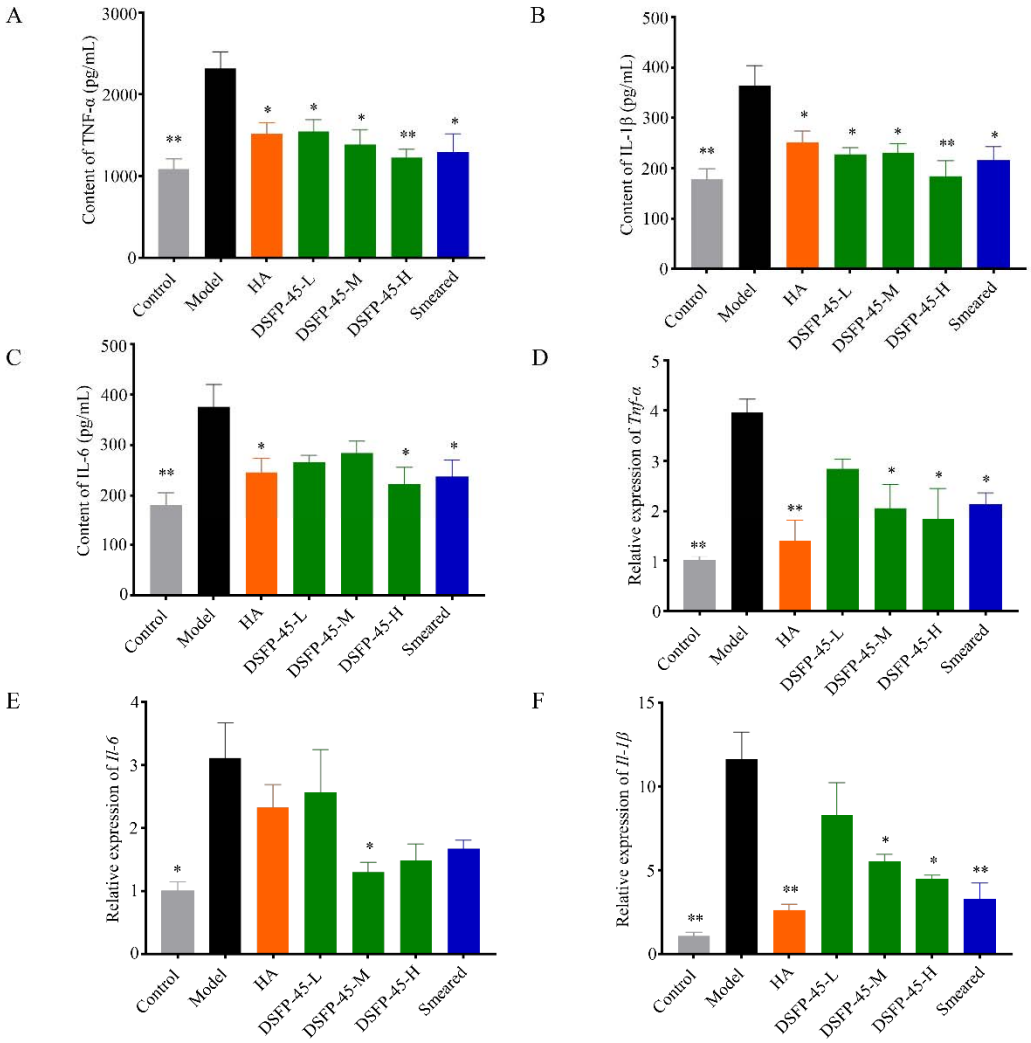

Figure 7. Effect of DSFP-45 on pro-inflammatory cytokines in photodamaged mice. (A) TNF- α contents; (B) IL-6 contents; (C) IL-1β contents; (D) Tnf- α expression; (G) Il-6 expression; (F) Il-1β expression.
Note: *, and ** indicate that other groups in the index have significant differences compared with the Model group.（$*P < 0.05$, $**P < 0.01$）. $^{\#}$, and $^{\#\#}$ indicate that other groups in the index have significant differences compared with group in same concentration.（$^{\#}P < 0.05$, $^{\#\#}P < 0.01$.

Consistent with protein expression, UVB irradiation significantly upregulated the gene expression levels of TNF-α, IL-1β, and IL-6 in the dorsal skin of mice in the Model group ($P < 0.05$, Figure 7D-F). Oral administration of DSFP-45 significantly downregulated these genes in a dose-dependent manner. Relative to the model group, DSFP-45 reduced TNF-α expression by 28.15%, 47.96%, and 54.06%; IL-1β by 29.13%, 52.42%, and 61.59%; and IL-6 decreased by 17.60%, 58.13%, and 52.22% at low, medium, and high doses, respectively. These findings demonstrate that DSFP-45 alleviates UVB-induced skin photodamage by suppressing pro-inflammatory cytokines expression and upregulating genes associated with skin barrier function within the experimental concentration range. Additionally, oral administration of DSFP-45 was more effective than topical application at equivalent dosage, highlighting its therapeutic potential. Notably, no significant dose-effect relationship was observed. At present, numerous studies have yet to determine the effect threshold of polysaccharides, and the dose-response effect of polysaccharides is not significant. This phenomenon may be attributed to several factors. First. polysaccharides can kill cells when present at high concentrations[40]. Second, the absorption of polysaccharides follows a non-linear pattern, and high

concentrations may even reduce the absorption amount[41]. Third, studies also show that polysaccharides with different structures exhibit different effects , and not every polysaccharide follows a linear dose-effect relationship[42, 43].

3.8 The effect of DSFP-45 on the skin microbiota of photodamaged mice

3.8.1 Species composition analysis

The effects of UVB irradiation and DSFP-45 treatment on skin microbiota were assessed by analyzing microbial abundance at different taxonomic levels. At the phylum level (Figure 8A), the skin microbiota was primarily composed of *Firmicutes, Proteobacteria, Actinobacteria, Bacteroideta, Patescibacteria* and *Cyanobacteria*. Among these, *Firmicutes, Proteobacteria* and *Actinobacterota* were dominant, accounting for 97% of the total bacterial population. UVB irradiation significantly decreased the relative abundance of *Firmicutes* decreased by 33.37%, while *Proteobacteria* and *Actinobacterota* increased by 24.77% and 5.03%, respectively, indicating disruption of the normal microbial community. After treatment with HA and medium dose of DSFP-45 significantly restored microbial balance by increasing *Firmicutes* and decreasing *Proteobacteria* and *Actinobacterota*, thereby shifting the microbiota composition closer to that of the control group.

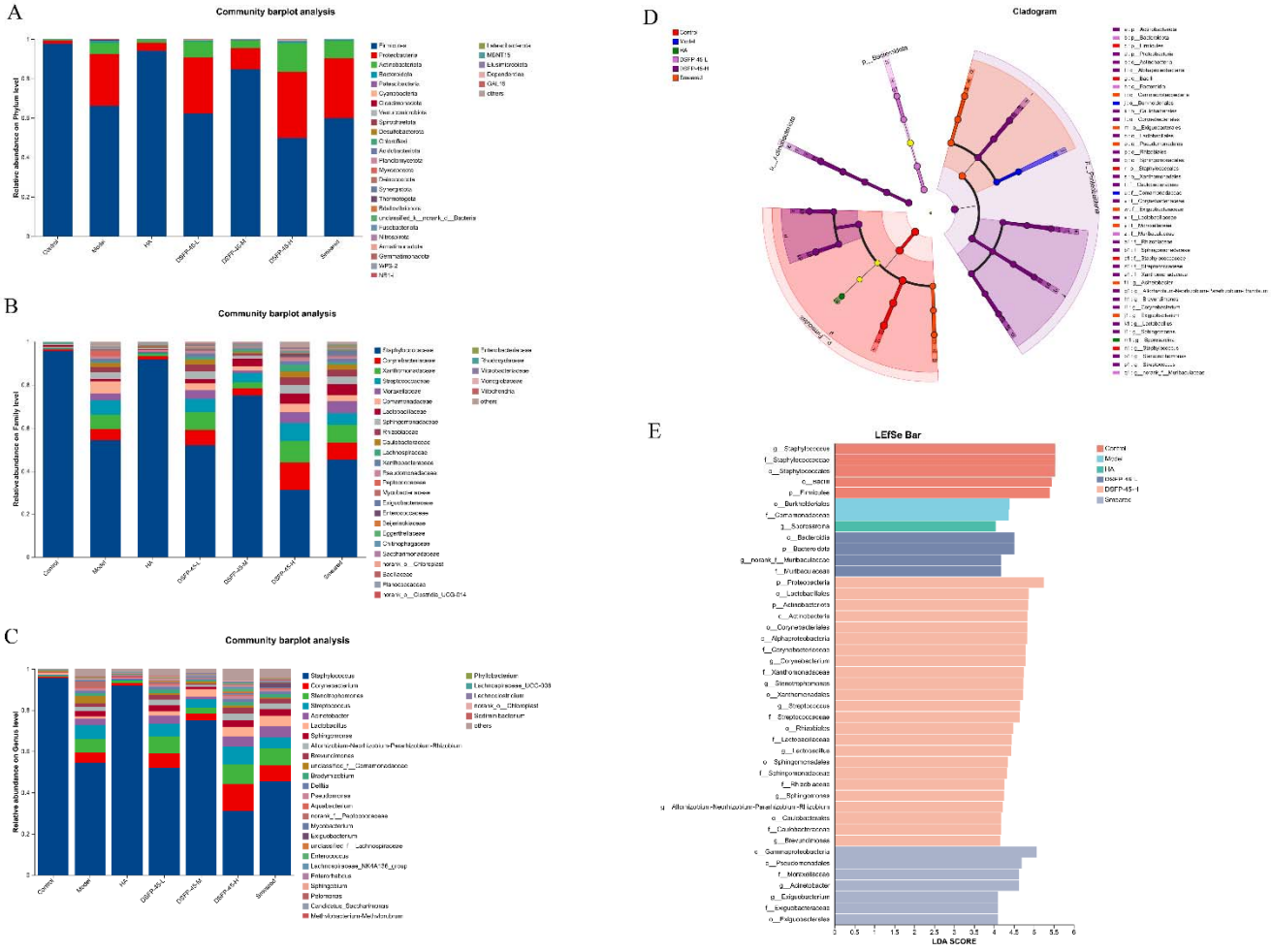

Figure 8. The effect of DSFP-45 on the microbiota species composition and species difference analysis of photodamaged mice. (A) phylum level; (B) family level; (C) genus leve (E) Cladogram of LEfSe analysis; (F) Histogram of the LDA scroes.

At the family level (Figure 8B), the predominant taxa included *Staphylococcus*, *Corynebacteriaceae*, *Xanthomonadaceae*, *Streptococcus*, *Moraxellaceae*, *Comamonadaceae* and *Lactobacillus*. Compared with the control group, the model group showed significant decreases in *Staphylococcus* and *Lactobacillus* in decreased significantly, while the relative abundance of *Corynebacteriaceae*, *Xanthomonadaceae*, *Streptococcaceae*, *Moraxellaceae* and *Comamonadaceae*. HA and medium dose of DSFP-45 treatment reversed these alterations, again restoring microbial structure toward the control group.

At the genus level (Figure 8C), *Staphylococcus*, *Corynebacterium*, *Stenotrophomonas*, *Streptococcus*, *Acinetobacter*, *Lactobacillus* and *Sphingomonas* dominated the skin microbiota. UVB irradiation significantly reduced *Staphylococcus* abundance, while *Corynebacterium*, *Stenotrophomonas*, *Streptococcus*, *Acinetobacter* and *Sphingomonas* increased in the model group. Consistent with the phylum and family level analyses, treatment with HA and medium doses DSFP-45 reversed these alterations, mitigating UVB-induced dysbiosis and restoring microbial community balance.

Obviously, DSFP-45 treatment significantly alters mouse skin microbial composition, likely due to skin environment restoration, reduced inflammation, and polysaccharide nutrient supply. Skin microbes depend on skin moisture for survival; Staphylococcus, for example, prefers a moist environment[44]. Oral and topical DSFP-45 increase skin TWEL and ceramide levels, maintaining moisture microbes need. Additionally, oral or topical polysaccharides lower inflammation. Studies show skin inflammation markedly affects skin microbial composition, though the mechanism is unclear[45]. Thus, this alteration may also stem from reduced inflammation. Finally, as a carbohydrate, polysaccharides are usable by microbes and promote microbial competition, ultimately altering composition[46]. Topical DSFP-45 may therefore change skin microbes by supplying energy. Generally, the skin microbiota is non-pathogenic. However, when the skin barrier is damaged, dysbiosis of the skin microbiota occurs, which can further contribute to the progression of skin diseases. Thus, the treatment of DSFP-45 may restore microbiota to prevent further progress of skin damage.

3.8.2 Analysis of Species Differences

The influence of microbial abundance on differential outcomes was analyzed using Linear discriminant analysis effect size (LEfSe) (Figure 8 E). LEfSe performs multi-level discriminant analysis to identify species contributing most to group differences, with linear discriminant analysis (LDA) values quantifying their impact (Figure 8 F). A higher LDA score indicate a stronger influence of that species on the observed differences, suggesting a potential key role in environmental change processes. As shown in Figure 9, species with with LDA values > 5 and $P < 0.05$ were screened, yielding 43 genera with intergroup differences. The Control group, Model group, HA group, DSFP-45-L group, DSFP-45-H group, and Smeared group were enriched with 5, 2, 1, 4, 24, and 7 differentially expressed microorganisms, respectively. Among them, the key representative species of the seven groups were *g_Staphylococcus*, *o__Burkholderiales*, *g__Sporosarcina*, *c__Bacteroidia*, *p__Proteobacteria* and *c__Gammaproteobacteria*, respectively. Microorganisms enriched in the Model group may serve as microbial markers of UVB induced skin photodamage, whereas the species

enriched in the DSFP-45-L treatment group may represent potential targets through which DSFP-45-H alleviates photodamage.

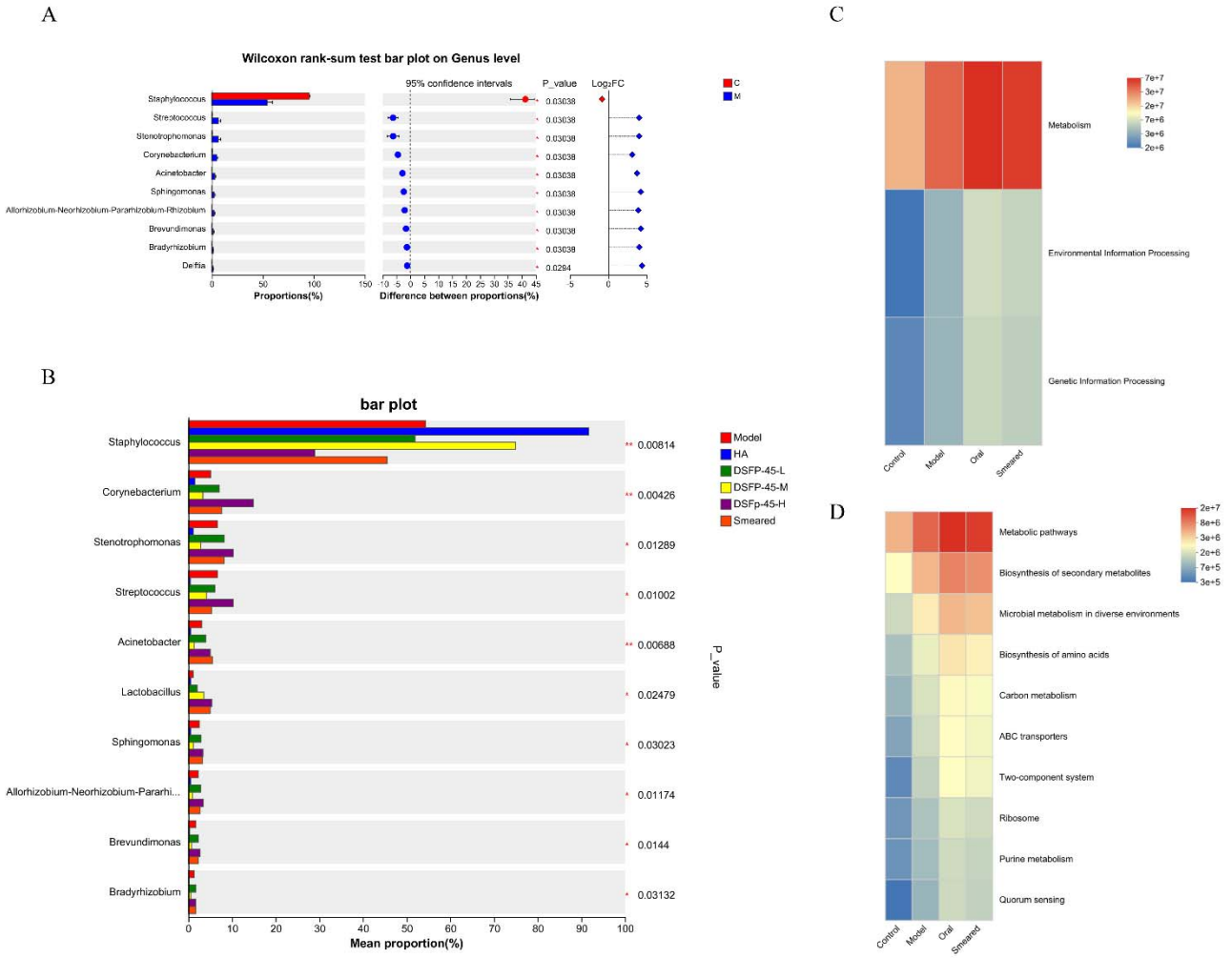

Figure 9. Comparison of species differences and KEGG pathways. (A) comparison between two groups (B) comparison among groups (C) level 1 (D) level 3.

Further we analyzed the top 10 taxa with the highest intergroup abundance between the control group and the model group, as well as between the Model group and the other treatment groups (Figure 9 A-B). Compared with the Control group, the Model group exhibited a marked reduction in *Staphylococcus* abundance, while significant increases in *Streptococcus*, *Stenotrophomonas* and *Corynebacterium*. UVB irradiation this substantially altered the microbial community structure of mice skin. Treatment with HA and medium doses DSFP-45 significantly restored *Staphylococcus* abundance, and increase *Lactobacilus*. partially re-establishing a healthy microbiota profile. Notably, *Staphylococcus epidermidis*, a major member of the *Staphylococcus* genus[47, 48], plays a crucial role in skin barrier protection and anti-inflammation. During inflammation, it activates TLR2 (Toll-like receptor 2) via Staphylococcal lipoteichoic acid to inhibit the inflammatory response[49]. Meanwhile, Staphylococcus epidermidis secretes antimicrobial peptides that inhibit certain pro-inflammatory pathogenic bacteria[49]. In addition, it secretes Sphingomyelinase with a specific structure, and this enzyme cleaves the membrane lipid sphingomyelin to produce ceramide without damaging host cells, thereby enhancing the moisture retention of the skin barrier[50]. Likewise, higher

Lactobacillus abundance has been associated with reduced skin inflammation, enhanced skin barrier function and improve skin health through immune regulation[51]. *Lactobacillus* inhibits skin inflammation via the recognition of its metabolites (e.g., Msp2/p40) or microbe-associated molecular patterns (MAMPs, such as pili) by Toll-like receptor (TLR) signaling[51]. *Corynebacterium* is dominant members of the skin microbiota. According to Ridaura et al.[6], under normal circumstances, *Corynebacterium* is non-pathogenic. However, when the skin barrier is impaired (as in the psoriasis model), *Corynebacterium* promotes skin inflammation. Specifically, its cell envelope mycolic acids are recognized by dendritic cells (DCs), which then secrete IL-23 to activate γδ T cells. This activation causes γδ T cells to produce IL-17, which further promotes skin inflammation. *Stenotrophomonas* is an opportunistic pathogen, which can cause primary cellulitis, metastatic cellulitis, and infectious mucocutaneous ulcers[7]. Additionally, *Streptococcus pyogenes* (a species within the genus *Streptococcus*) is an invasive bacterial pathogen. On the skin, it secretes the streptolysin S to activates TRPV1 neurons to induce pain. Subsequently, nociceptors release neuropeptide calcitonin gene-related peptide, which inhibits neutrophil recruitment (key for host defense) and their bactericidal activity. This thereby enhances *Streptococcus pyogenes* survival in invasive infections[52]. *Stenotrophomonas maltophilia*, a major *Stenotrophomonas* species, is an emerging opportunistic pathogen and highly drug-resistant[53]. When the skin barrier is impaired, the host becomes highly susceptible to infection, which can cause skin and soft tissue inflammation, even death[54]. In summary, DSFP-45 alleviates UVB-induced dysbiosis by modulating the abundance of key taxa, particularly through upregulating beneficial bacteria such as *Staphylococcus* and *Lactobacilus* ,and downregulating harmful bacteria sucha as *Corynebacterium*, *Stenotrophomonas* and *Streptococcus*. This microbial regulation may contribute to its anti-photodamage effects.

3.8.3 Predicted functional changes in the skin microbiota

KEGG is an integrated database composed of three distinct levels, which systematically documents the connections between genomes, biological pathways, and diseases. Therefore, the present study performed PICRUSt2 and KEGG analyses to predict the metabolic functions based on the microbiome metagenome.

At the level 1 of KEGG metabolic pathways (Figure 9 C), compared with the Control group , the Metabolism, Environmental Information Processing, and Genetic Information Processing pathways were significantly enhanced in Model group, Oral group, and Smeared group. At the level 3 (Figure 9 D), relative to Control group, Model group, Oral group, and Smeared group exhibited remarkable enhancement in the functions of Biosynthesis of amino acids, Carbon metabolism, ABC transporters, Two-component system, Ribosome, Purine metabolism, and Quorum sensing. This observation can be attributed to the fact that UV irradiation tends to enrich bacteria with strong UV resistance[55]. To cope with UV exposure, these bacteria enhance their carbon metabolism capacity to increase energy supply. Additionally, such bacteria can counteract UV-induced damage through DNA repair mechanisms, production of antioxidant enzymes [56]. Compared with the model group, the biosynthesis of secondary metabolites is enhanced. Metabolites of the skin microbiota, such as short-chain fatty acids and indole derivatives, play a key role in skin pH stabilization and skin barrier repair[57]. Notably, N-Formylmethionine (fMet) peptides essential for bacterial protein

translation. These fMet peptides produced by *Staphylococcus epidermidis* were recognized by dendritic cells, which induces CD8 T cells to express abundant tissue repair-related transcripts and promote skin repair[59]. Two key observations are considered. One is requirement of protein translation for bacterial repair and the enhanced biosynthesis of amino acids compared with Model group. The other is the previously mentioned increased relative abundance of *Staphylococcus* in the polysaccharide-treated group. It is thus infer that *Staphylococcus* with higher relative abundance in this group exerts a positive effect on skin repair.

4. Conclusion

Excessive UV irradiation would cause skin photodamage and inflammation, affecting human health. The experimental results of HaCaT cells and nude mice undergoing photodamage showed that after UVB irradiation, the skin barrier function of mice was impaired, and TEWL increased, leading to excessive dehydration of the skin. Meanwhile, the levels of pro-inflammatory cytokines (TNF-α, IL-6, IL-1β) increased. DSFP-45 improved skin barrier damage by upregulating the contents and expression of FLG, LOR and AQP3 barrier functional proteins in HaCaT cells and nude mouse skin. DSFP-45 reduced skin moisture loss by increasing moisturizing factors and ceramide content. *Bacillus* flora. At the same time, DSFP-45 could also protect the skin barrier and reduce skin photodamage by maintaining the normal shape of elastic fibers, and possibly by increasing the relative abundance of *Staphylococcus* and *Lactobacillus* flora, and decreasing the relative abundance of *Corynebacterium*, *Streptococcus*, and *Streptococcus* flora. KEGG metabolic pathway analysis showed that the skin microbiota under DSFP-45 treatment influence biosynthesis of amino acids and biosynthesis of secondary metabolites. In conclusion, DSFP-45 inhibits the skin-inflammation vicious cycle and protects against UVB-induced skin damage by alleviating barrier damage, reducing skin inflammation, and potentially modulating the microbiota. Future studies could further verify the role of skin microbiota in alleviating UVB irradiation-induced damage, so as to provide insights into the polysaccharide-skin microbiota-skin axis.

Declaration of competing interest

The authors declare that they have no conflicts of interest regarding the research presented in this manuscript.

Acknowledgment

This research was funded by the National Key Research and Development Program of China (2024YFF1106000), the Guangdong Basic and Applied Basic Research Foundation (2023B1515040014) and National Natural Science Foundation of China (22278153).

References

[1] X. Tang, T. Yang, D. Yu, et al., Current insights and future perspectives of ultraviolet radiation (UV) exposure: Friends and foes to the skin and beyond the skin, Environ. Int. 185 (2024) 108535. https://doi.org/10.1016/j.envint.2024.108535.

[2] G. Zhou, L. Peng, W. Gao, et al., The acute effects of ultraviolet radiation exposure on solar dermatitis in Shanghai, China, Int. J. Biometeorol. 64 (2020) 585-591. https://doi.org/10.1007/s00484-019-01845-4.

[3] F. Awad, E. Assrawi, C. Louvrier, et al., Photoaging and skin cancer: Is the inflammasome the missing link?, Mech. Ageing Dev. 172 (2018) 131-137. https://doi.org/10.1016/j.mad.2018.03.003.

[4] F. Wellen, S.T. Tan, Y. Firmansyah, et al., Correlation between facial skin damage due to UV exposure and facial skin porphyrin level: Study on students of SMA Kalam Kudus II Jakarta, Indonesia, Bioscientia Medicina: J. Biomedicine Transl. Res. 6 (18) (2023) 2948-2952. https://doi.org/10.37275/bsm.v6i18.737.

[5] G. Yang, J.K. Seok, H.C. Kang, et al., Skin Barrier Abnormalities and Immune Dysfunction in Atopic Dermatitis, Int. J. Mol. Sci. 21 (8) (2020) 2867. https://doi.org/10.3390/ijms21082867.

[6] V.K. Ridaura, N. Bouladoux, J. Claesen, et al., Contextual control of skin immunity and inflammation by *Corynebacterium*, J. Exp. Med. 215 (3) (2018) 785-799. https://doi.org/10.1084/jem.20171079.

[7] W.Y. Teo, M.Y. Chan, C.M. Lam, et al., Skin manifestation of Stenotrophomonas maltophilia infection--a case report and review article, Ann. Acad. Med. Singap. 35 (2006) 897-900.

[8] B.E. Kim, M.D. Howell, E. Guttman-Yassky, et al., TNF-α downregulates filaggrin and loricrin through c-Jun N-terminal kinase: role for TNF-α antagonists to improve skin barrier, J. Invest. Dermatol. 131 (6) (2011) 1272-1279. https://doi.org/10.1038/jid.2011.24.

[9] Y. Fu, H. Jiao, J. Sun, et al., Structure-activity relationships of bioactive polysaccharides extracted from macroalgae towards biomedical application: A review, Carbohydr. Polym. 324 (2024) 121533. https://doi.org/10.1016/j.carbpol.2023.121533.

[10] L. Wang, J.Y. Oh, H.S. Kim, et al., Protective effect of polysaccharides from Celluclast-assisted extract of Hizikia fusiforme against hydrogen peroxide-induced oxidative stress in vitro in Vero cells and in vivo in zebrafish, Int. J. Biol. Macromol. 112 (2018) 483-489. https://doi.org/10.1016/j.ijbiomac.2018.01.212.

[11] X. Chen, W. Nie, S. Fan, et al., A polysaccharide from *Sargassum fusiforme* protects against immunosuppression in cyclophosphamide-treated mice, Carbohydr. Polym. 90 (2) (2012) 1114-1119. https://doi.org/10.1016/j.carbpol.2012.06.052.

[12] Q. Cong, F. Xiao, W. Liao, et al., Structure and biological activities of an alginate from *Sargassum fusiforme*, and its sulfated derivative, Int. J. Biol. Macromol. 69 (2014) 252-259. https://doi.org/10.1016/j.ijbiomac.2014.05.056.

[13] S. Chang, Y. Chen, H. Qiu, et al., The isolation, structure characterizations and anti-photoaging activities of sulfated polysaccharides isolated from *Sargassum fusiforme*, Chem. Biol. Technol. Agric. 11 (2024) 64. https://doi.org/10.1186/s40538-024-00587-9.

[14] R.B. Jia, Z.R. Li, J. Wu, et al., Physicochemical properties of polysaccharide fractions from *Sargassum fusiforme* and their hypoglycemic and hypolipidemic activities in type 2 diabetic rats, Int. J. Biol. Macromol. 147 (2020) 428-438. https://doi.org/10.1016/j.ijbiomac.2019.12.243.

[15] J. Hu, W. Yao, S. Chang, et al., Structural characterization and anti-photoaging activity of a polysaccharide from *Sargassum fusiforme*, Food Res. Int. 157 (2022) 111267. https://doi.org/10.1016/j.foodres.2022.111267.

[16] W. Yao, J. Yong, B. Lv, et al., Enhanced In Vitro Anti-Photoaging Effect of Degraded Seaweed Polysaccharides by UV/H(2)O(2) Treatment, Mar Drugs. 21(8) (2023) 430. https://doi.org/10.3390/md21080430.

[17] W. Z. Yao, J. Yong, B. Lv, et al., Enhanced In Vitro Anti-Photoaging Effect of Degraded Seaweed Polysaccharides by UV/H2O2 Treatment, Mar. Drugs. 21(8) (2023) 430. https://doi.org/10.3390/md21080430.

[18] W. Yao, X. Chen, X. Li, et al., Current trends in the anti-photoaging activities and mechanisms of dietary non-starch polysaccharides from natural resources, Crit. Rev. Food Sci. Nutr. 62 (2022) 9021-9035. https://doi.org/10.1080/10408398.2021.1939263.

[19] N. Chen, T.Y. Jiang, J.X. Xu, et al., The relationship between polysaccharide structure and its antioxidant activity needs to be systematically elucidated, Int. J. Biol. Macromol. 270 (2024) 132391. https://doi.org/10.1016/j.ijbiomac.2024.132391.

[20] Y. Kim, K.M. Lim, Skin barrier dysfunction and filaggrin, Arch. Pharmacal Res. 44(1) (2021) 36-48. https://doi.org/10.1007/s12272-021-01305-x.

[21] C.R. Harding, S. Aho, C.A. Bosko, Filaggrin – revisited, Int. J. Cosmet. Sci. 35(5) (2013) 412-423. https://doi.org/10.1111/ics.12049.

[22] Y. Morishita, Y. Sakube, S. Sasaki, et al., Molecular mechanisms and drug development in aquaporin water channel diseases: Aquaporin superfamily (superaquaporins): Expansion of aquaporins restricted to multicellular organisms, J. Pharmacol. Sci. 96(3) (2004) 276-279. https://doi.org/10.1254/jphs.FMJ04004X7.

[23] M.K. Kang, D.Y. Kim, H. Oh, et al., Dietary collagen hydrolysates ameliorate furrowed and parched skin caused by photoaging in gairless mice, Int. J. Mol. Sci. 22(11) (2021) 6137. https://doi.org/10.3390/ijms22116137.

[24] E. Sawada, N. Yoshida, A. Sugiura, et al., Th1 cytokines accentuate but Th2 cytokines attenuate ceramide production in the stratum corneum of human epidermal equivalents: An implication for the disrupted barrier mechanism in atopic dermatitis, J. Dermatol. Sci. 68(1) (2012) 25-35. https://doi.org/10.1016/j.jdermsci.2012.07.004.

[25] S. T. Li, Ultraviolet-induced skin barrier damage and its correlation with immune response, Kunming Medical University, 2015.

[26] J.M. Janus, R.F.L. O'Shaughnessy, C.A. Harwood, et al., Phosphoinositide 3-kinase-dependent signalling pathways in cutaneous squamous Cell Carcinomas, Cancers 9(7) (2017) 86. https://doi.org/10.3390/cancers9070086.

[27] Q. X. Xiong, Regulatory effect of PI3K/AKT/NF-KB signaling pathway on HIF-1α expression in bone marrow tissue of rats with high altitude polycythemia, Sichuan Agricultural University, 2018.

[28] T. Omotezako, W.Z. Zhao, M. Rodrigues, et al., Skin inflammatory signatures, as measured by disordered spatial redness patterns, predict current and future skin ageing attributes, Exp. Dermatol. 33(8) (2024) e15163. https://doi.org/10.1111/exd.15163.

[29] M. Akdeniz, S. Gabriel, A. Lichterfeld-Kottner, et al., Transepidermal water loss in healthy adults: a systematic review and meta-analysis update, Br. J. Dermatol. 179(5) (2018) 1049-1055. https://doi.org/10.1111/bjd.17025.

[30] W. J. Sim, E. Lee, G. Lee, et al., Inhibition of photoaging by anthocyanin metabolites derived from rose petal extract, Mol. Nutr. Food Res. 68(5) (2024) 2300611. https://doi.org/10.1002/mnfr.202300611.

[31] Z. Li, R. Jiang, M. Wang, et al., Ginsenosides repair UVB-induced skin barrier damage in BALB/c hairless mice and HaCaT keratinocytes, J. Ginseng Res. 46(1) (2022) 115-125. https://doi.org/10.1016/j.jgr.2021.05.001.

[32] H. Xie, L. Zhou, F. Liu, et al., Autophagy induction regulates aquaporin 3-mediated skin fibroblast ageing, Br. J. Dermatol. 186(2) (2022) 318-333. https://doi.org/10.1111/bjd.20662.

[33] S. Park, E.S. Lee, N.H. Park, et al., Circadian expression of TIMP3 is disrupted by UVB irradiation and recovered by green tea extracts, Int. J. Mol. Sci. 20(4) 2019 862. https://doi.org/10.3390/ijms20040862.

[34] C.J. van der Vleuten, E.J. Kroot, E.M. de Jong, et al., The immunohistochemical effects of a single challenge with an intermediate dose of ultraviolet B on normal human skin, Archives of dermatological research. 288 (1996) 510-516. https://doi.org/10.1007/bf02505246.

[35] S. Y. Choi, B. H. Bin, W. Kim, et al., Exposure of human melanocytes to UVB twice and subsequent incubation leads to cellular senescence and senescence-associated pigmentation through the prolonged p53 expression, Journal of Dermatological Science. 90 (2018) 303-312. https://doi.org/https://doi.org/10.1016/j.jdermsci.2018.02.016.

[36] X. Zheng, W. Bollinger Bollag, Aquaporin 3 Colocates with Phospholipase D2 in Caveolin-Rich Membrane Microdomains and Is Downregulated Upon Keratinocyte Differentiation, Journal of Investigative Dermatology. 121 (2003) 1487-1495. https://doi.org/https://doi.org/10.1111/j.1523-1747.2003.12614.

[37] A. Gęgotek, W. Łuczaj, E. Skrzydlewska, Effects of natural antioxidants on phospholipid and ceramide profiles of 3D-Cultured skin fibroblasts exposed to UVA or UVB radiation, Antioxidants. 10(4) 2021 578. https://doi.org/10.3390/antiox10040578.

[38] Y. Uchida, A.D. Nardo, V. Collins, et al., De novo ceramide synthesis participates in the ultraviolet B irradiation-induced apoptosis in undifferentiated cultured human keratinocytes, J. Invest. Dermatol. 120(4) (2003) 662-669. https://doi.org/10.1046/j.1523-1747.2003.12098.x.

[39] N. Dalmau, N. Andrieu-Abadie, R. Tauler, et al., Phenotypic and lipidomic characterization of primary human epidermal keratinocytes exposed to simulated solar UV radiation, J. Dermatol. Sci. 92(1) (2018) 97-105. https://doi.org/10.1016/j.jdermsci.2018.07.002.

[40] G. Pang, F. Wang, L.W. Zhang, Dose matters: Direct killing or immunoregulatory effects of natural polysaccharides in cancer treatment, Carbohydr. Polym. 195 (2018) 243-256. https://doi.org/10.1016/j.carbpol.2018.04.100.

[41] Z. Zheng, X. Pan, L. Luo, et al., Advances in oral absorption of polysaccharides: Mechanism, affecting factors, and improvement strategies, Carbohydr. Polym. 282 (2022) 119110. https://doi.org/10.1016/j.carbpol.2022.119110.

[42] M.-T. Qiu, L. Zhou, X.-Y. Wang, et al., Anti-colitis comparison of polysaccharides and anthocyanins extracted from black wolfberry based on microbiomics, immunofluorescence and multi-cytokines profile analysis, Int. J. Biol. Macromol. 310 (2025) 143700. https://doi.org/10.1016/j.ijbiomac.2025.143700.

[43] Y. Qiu, A. Zhang, X. Lian, et al., Unraveling the link between structural properties of polysaccharides and anti-inflammatory activity: A review, Carbohydr. Res. 555 (2025) 109583. https://doi.org/10.1016/j.carres.2025.109583.

[44] T.A. Harris-Tryon, E.A. Grice, Microbiota and maintenance of skin barrier function, Science. 376(6596) (2022) 940-945. https://doi.org/10.1126/science.abo0693.

[45] Y.E. Chen, M.A. Fischbach, Y. Belkaid, Skin microbiota–host interactions, Nature. 553 (2018) 427-436. https://doi.org/10.1038/nature25177.

[46] S. Cui, M. Pan, X. Tang, et al., Metagenomic insights into the effects of cosmetics containing complex polysaccharides on the composition of skin microbiota in females, Front. Cell. Infect. Microbiol. 13 (2023) 1210724. https://doi.org/10.3389/fcimb.2023.1210724.

[47] S. Keshari, A. Balasubramaniam, B. Myagmardoloonjin, et al., Butyric acid from probiotic *Staphylococcus epidermidis* in the skin microbiome down-regulates the ultraviolet-induced pro-inflammatory IL-6 cytokine via short-chain fatty acid receptor, Int. J. Mol. Sci. 20(18) (2019) 4477. https://doi.org/10.3390/ijms20184477.

[48] T. Nakatsuji, T.H. Chen, A.M. Butcher, et al., A commensal strain of Staphylococcus epidermidis protects against skin neoplasia, Sci. Adv. 4 (2018) eaao4502. https://doi.org/10.1126/sciadv.aao4502.

[49] A. Stacy, Y. Belkaid, Microbial guardians of skin health, Science. 363(6424) (2019) 227-228. https://doi.org/10.1126/science.aat4326.

[50] Y. Zheng, R.L. Hunt, A.E. Villaruz, et al., Commensal Staphylococcus epidermidis contributes to skin barrier homeostasis by generating protective ceramides, Cell Host Microbe. 30(3) (2022) 301-313.e309. https://doi.org/10.1016/j.chom.2022.01.004.

[51] L. Delanghe, I. Spacova, J. Van Malderen, et al., The role of lactobacilli in inhibiting skin pathogens, Biochem. Soc. Trans. 49(2) (2021) 617-627. https://doi.org/10.1042/bst20200329.

[52] F.A. Pinho-Ribeiro, B. Baddal, R. Haarsma, et al., Blocking neuronal signaling to immune cells treats streptococcal invasive infection, Cell 173(5) (2018) 1083-1097. https://doi.org/10.1016/j.cell.2018.04.006.

[53] R.P. Ryan, S. Monchy, M. Cardinale, et al., The versatility and adaptation of bacteria from the genus Stenotrophomonas, Nat. Rev. Microbiol. 7 (2009) 514-525. https://doi.org/10.1038/nrmicro2163.

[54] A. Belzer, E. Weiss, F. Etaee, et al., Stenotrophomonas maltophilia, a Pathogen of Increasing Relevance to Dermatologists: A Case Report and Review of the Literature, Antibiotics (Basel). 11(10) (2022) 1398. https://doi.org/10.3390/antibiotics11101398.

[55] N. Harel, N. Ogen-Shtern, L. Reshef, et al., Skin microbiome bacteria enriched following long sun exposure can reduce oxidative damage, Res. Microbiol. 174(8) (2023) 104138. https://doi.org/10.1016/j.resmic.2023.104138.

[56] K.L. Nelson, A.B. Boehm, R.J. Davies-Colley, et al., Sunlight-mediated inactivation of health-relevant microorganisms in water: a review of mechanisms and modeling approaches, Environ. Sci. Process Impacts. 20 (2018) 1089-1122. https://doi.org/10.1039/c8em00047f.

[57] H.B. Kim, H. Alexander, J.Y. Um, et al., Skin Microbiome Dynamics in Atopic Dermatitis: Understanding Host-Microbiome Interactions, Allergy, Asthma Immunol. Res. 17 (2025) 165-180. https://doi.org/10.4168/aair.2025.17.2.165.

[58] J.L. Linehan, O.J. Harrison, S.-J. Han, et al., Non-classical Immunity Controls Microbiota Impact on Skin Immunity and Tissue Repair, Cell. 172 (2018) 784-796. https://doi.org/10.1016/j.cell.2017.12.033.